https://doi.org/10.5194/esurf-2019-78
Preprint. Discussion started: 4 February 2020

Earth Surface Dynamics Discussions
Open Access
EGU

State of the Art Study of Influence of Bed Roughness and Alluvial Cover on Bedrock Channels and Comparisons of Existing Models with Laboratory Scale Experiments

Jagriti Mishra[1], Takuya Inoue[1]

[1] Civil Engineering Research Institute for Cold Region, Sapporo-Hokkaido, Japan

Correspondence to: Jagriti Mishra (jagritimp@gmail.com)

Abstract. Several studies have implied towards the importance of bed roughness on alluvial cover, besides, several mathematical models have also been introduced to mimic the effect bed roughness may project on alluvial cover. Here, we provide a state of the art review of research exploring the relationship between alluvial cover, sediment supply and bed topography, thereby, describing various mathematical models used to analyse deposition of alluvium. In the interest of analysing the efficiency of various available mathematical models, we performed laboratory-scale experiments and compared the results with various models. Our experiments show that alluvial cover is not merely governed by increasing sediment supply, and, bed topography is an important controlling factor of alluvial cover. Testing experimental results with various theoretical models suggest a fit of certain models for a particular bed topography and inefficiency in predicting higher roughness topography. Three models efficiently predict the experimental observations, albeit their limitations which we discuss here in detail.

1 Introduction

Economic growth worldwide has fuelled the demand for the construction of straightened river channels, sabo dams, the collection of gravel samples for various research, etc.; leading to a decline in sediment availability and alluvial bed cover. Sediment availability has two contradicting effects on the river bed (Gilbert, 1877; Sklar and Dietrich, 1998; Johnson et al., 2010; Mishra et al., 2018). It acts as a tool and erodes the bedrock bed, known as tools effect. As sediment availability becomes larger than sediment transport capacity of the channel, the sediment starts settling down on the river bed providing a cover for the bed underneath from further erosion, known as the cover effect. Various studies have established the importance of alluvial cover in moderating bedrock incision and shape. Finnegan et al. (2007) conducted laboratory-scale experiments and studied the interdependence among incision, bed roughness and alluvial cover. Their results indicated that alluvial deposition on the bed shifted bed erosion to higher regions of the channel or bank of the channel. Cowie et al. (2008) and Mishra et al. (2018) showed that incision rate increased when the sediment supply rate of the channel became considerably smaller than the sediment carrying capacity of the channel. Johnson et al. (2009) surveyed the Henry Mountains in Utah and suggested that alluvial cover does not only inhibit bed erosion for a covered bed but also when the bedrock bed is exposed in some parts.

https://doi.org/10.5194/esurf-2019-78
Preprint. Discussion started: 4 February 2020


Earth Surface Dynamics Discussions
Open Access
EGU

Flume studies conducted by Johnson et al. (2010) have shown the importance of alluvial cover in regulating the roughness of bedrock bed by providing a cover for the local lows and thereby inhibiting the erosion and focusing erosion on local highs. Yanites et al. (2011) studied the changes in Peikang River in central Taiwan triggered by the thick sediment cover introduced by landslides and typhoons during the 1999 Chi-Chi earthquake. Their results show slowed or no incision in high transport capacity and low transport capacity channels. Inoue et al. (2014) conducted experiments by excavating channel into natural bedrocks in Ishikari River, Asahikawa, Hokkaido – Japan. They suggested that the erosion rate in cover-free sections was positively associated with the sediment supply rate. They also advocated an interaction between alluvial cover and bed roughness such that when alluvial cover decreases the bed roughness increases.

According to saltation-abrasion model proposed by Sklar and Dietrich (2004) the bedrock exposure decreases linearly with the ratio of sediment flux to sediment transport capacity. Their cover model can be expressed as the following equation

$$P_c = \begin{cases} q_{bs}/q_{bc} & for\ \ 0 \le q_{bs}/q_{bc} \le 1 \\ 1 & for\ \ q_{bs}/q_{bc} > 1 \end{cases} \quad (1)$$

where, P_c is the mean areal fraction of alluvial cover, q_{bs} and q_{bc} are the volume sediment supply rate per unit width and transport capacity, respectively. The value of P_c i.e. the alluvial cover ratio is 1 when the sediment supply is larger than the transport capacity, the gravel cover does not decrease as the sediment gets deposited on the bed, consequently, the bedrock is not exposed. If there is no sediment supply, the gravel deposit will disappear and eventually the bedrock bed will be completely exposed and P_c will be equal to 0. Laboratory scale studies conducted by Chatanantavet and Parker (2008) and Johnson and Whipple (2010) mostly support the cover model proposed by Sklar and Dietrich (2004). Chatanantavet and Parker (2008) conducted laboratory-scale experiments in straight concrete bedrock channels with varying bedrock roughness and evaluated bedrock exposure with respect to sediment availability. In their experiments, alluvial cover increased linearly with increasing sediment supply in case of higher bed roughness, whereas in case of lower bed roughness and higher slopes, the bed shifted abruptly from being completely exposed to being completely covered. Hodge and Hoey (2016a) conducted laboratory-scale experiments in a 3D printed flume of natural stream Trout Beck, North Pennies-U.K. Their first set of experiments focused on quantifying hydraulic change with varying discharge, suggesting that hydraulic properties fluctuate more during higher discharge. Their second set of experiments (Hodge and Hoey, 2016b) concentrated on quantifying the sediment dynamics for varying discharge and sediment supply. They supplied 4 kg and 8 kg of sediment pulse to the channel and observed a similar alluvial pattern in both cases suggesting that the deposition of sediment on the bed may not only depend on the amount of sediment supplied, but may be strongly influenced by the bed topography. In order to express the non-linear relationship between P_c and q_{bs}/q_{bc}, Turowski et al. (2007) proposed a model that considered the cover effect as an exponential function of the ratio of sediment flux to sediment transport capacity. Turowski et al.'s model can be expressed as the following equation

$$P_c = 1 - \exp\left(-\varphi \frac{q_{bs}}{q_{bc}}\right) \quad (2)$$

where, φ is a dimensionless cover factor parameter and determines sediment deposition on covered areas for $\varphi < 1$ and deposition on uncovered areas for $\varphi > 1$ (Turowski et al., 2007; Turowski, 2009). Hodge et al. (2011) reported different types

https://doi.org/10.5194/esurf-2019-78
Preprint. Discussion started: 4 February 2020


Earth Surface Dynamics Discussions
Open Access
EGU

of sediment cover from three rivers, River Calder, South Fork Eel River and Allt Dubhaig river. They contributed the formation and change in sediment cover to grain entrainment (E), translation caused by saltation (T) and deposition (D), combined together, cast E-T-D effect on a grain. They showed that grain deposition on a bedrock surface is unlikely and entrainment of grains on a bedrock surface occurs at a lower shear stress. Whereas, in case of alluvial surface grain deposition is more favourable. They advocated the need for models that focus on the cover extent and depth to understand sediment processes. Hodge and Hoey (2012) introduced Cellular Automaton Model that assigned an entrainment probability to each grain. The assigned probability of each grain was decided by the number of neighbouring cells containing a grain. If five or more of total eight neighbouring cells contained grain, the grain was considered to be a part of the cover, otherwise, it was considered an isolated grain. They suggested that runaway alluviation occurred only in cases when isolated grains were more than the cover on the bed. Also, they advised a sigmoidal relationship between q_{bs}/q_{bc} and $1 - P_c$. Aubert et al., in 2016 proposed a Discrete-Element Model where $q_{bs} = N[\pi(d/2)^2/wl]$ where N is the number of spherical grain, d is the grain size, w and l represent the width and length of the flume respectively. They determined P_c from the velocity distribution of the grains. If the velocity of a grain is $1/10^{th}$ or lower than the maximum velocity, the grain settles as cover on the bedrock surface. The model, however cannot deal with non-uniform velocity fields and hence cannot predict results for varying alluvial cover. Recently, Johnson (2014) and Inoue et al. (2014) proposed physically-based models that could encompass the effects of bed roughness and sediment flux. Turowski and Hodge (2017) proposed probability based model that can deal with evolution of cover residing on the bed and the exposed bedrock.

In this study, we provide a detailed study of the similarities and differences among the models proposed by Sklar and Dietrich (2004), Turowski et al. (2007), Inoue et al. (2014), Johnson (2014) and Turowski and Hodge (2017). We compare the efficacy of these models from comparisons with our experimental results. For better insight, we also test these models for prediction of experiments conducted by Chatanantavet and Parker (2008).

1.1 Bedrock Models governing consequences of roughness and sediment flux

Inoue et al. (2014) conducted several experiments by excavating a channel into a natural bedrock at Ishikari River in Japan. They conducted experiments with different combinations of flow discharge, sediment supply rate, grain size and roughness. Their experiments advocated that the dimensionless critical shear stress is related to the roughness of the channel. Their experiments also suggested that with an increase in alluvial cover, the bedrock bed roughness decreases, also, erosion in areas with an exposed bed is proportionate to sediment flux. They also conceptualised 'Clast Rough' and 'Clast Smooth' bedrock surfaces. A bedrock surface is clast-rough when bedrock hydraulic roughness is greater than the alluvial bed hydraulic roughness (supplied sediment), otherwise, a surface is clast-smooth i.e. when the bedrock roughness is lower than the alluvial roughness.

These experimental results motivated their mathematical model formulating the interaction between alluvial cover, dimensionless critical shear stress, transport capacity and the ratio of bedrock hydraulic roughness to alluvial hydraulic roughness. They calculated total hydraulic roughness height (k_s) as a function of alluvial cover:

https://doi.org/10.5194/esurf-2019-78
Preprint. Discussion started: 4 February 2020

Earth Surface Dynamics Discussions
Open Access
EGU

$$k_s = \begin{cases} (1-P_c)k_{sb} + (P_c)k_{sa} & for\ 0 \le P_c \le 1 \\ k_{sa} & for\ P_c > 1 \end{cases} \quad (3)$$

where k_s is the total hydraulic roughness height of bedrock channel, P_c is the cover fraction calculated as proposed by Parker et al. (2013) depends on ratio η_a/L where ηa is the alluvial cover thickness and L is the macro-roughness height. k_{sb} and k_{sa} represent the hydraulic roughness height of bedrock and alluvial bed respectively. The total transport capacity per unit width q_{bc} in Inoue et al.'s model is calculated as follows:

$$q_{bc} = \alpha(\tau_* - \tau_{*c})^{1.5}\sqrt{Rgd^3} \quad (4)$$

$$\tau_{*c} = 0.027(k_s/d)^{0.75} \quad (5)$$

where α is a bedload transport coefficient taken as 2.66 in this study, τ_* and τ_{*c} are the dimensionless shear stress and dimensionless critical shear stress, R is the specific gravity of the sediment in water (1.65), g is the gravitational acceleration and d is the particle size. In this model, P_c is back-calculated from Equations (3), (4) and (5) under the assumption that the sediment supply rate q_{bs} and the sediment transport capacity q_{bc} are balanced in dynamic equilibrium state.

The sensitivity analysis of bedrock roughness and sediment supply rate conducted by Inoue et al. (2014) showed that for a given sediment supply, the deposition is higher when bedrock roughness is larger. They also showed that clast-smooth surface shows a sudden transition from completely exposed bedrock to completely alluvial, also, clast-smooth surfaces show runaway alluviation. Johnson (2014) proposed a roughness model using the median diameter grain size. They also calculated the hydraulic roughness using the aerial alluvial cover fraction.

$$k_{sa} = r_d d[1 + (k_{\#D} - 1)P_c] \quad (6)$$

where $r_d = 2$ is a coefficient and $k_{\#D}$ is called a non-dimensional alluvial roughness representing variations in topography. The bedrock hydraulic roughness $k_{sb} = r_d r_{br}\sigma_{br}$ where r_{br} is a scaling parameter for bedrock roughness to grain roughness and σ_{br} is the bedrock surface roughness. Their model calculates bedrock shear stress using Wilcock and Crowe (2003) hiding/exposure function (b_r), modified to depend on a standard deviation of bedrock elevations and a bedrock roughness scaling parameter. Johnson (2014) calculated the total transport capacity using bedload equations proposed by Meyer-Peter and Müller (1948) and Wilcock and Crowe (2003). Here we introduce Meyer-Peter and Müller (MPM) based Johnson's model:

$$q_{bc} = (1-P_c)q_{bcb} + (P_c)q_{bca} \quad (7)$$

$$q_{bca} = \alpha(\tau_* - \tau_{*c})^{1.5}\sqrt{Rgd^3} \quad (8)$$

$$q_{bcb} = \alpha(\tau_* - \tau_{*cb})^{1.5}\sqrt{Rgd^3} \quad (9)$$

$$\tau_{*cb} = \frac{\tau_{*c} r_{br}\sigma_{br}}{d}\left(\frac{d}{r_{br}\sigma_{br}}\right)^{b_r} \quad (10)$$

$$b_r = \frac{0.67}{1+exp(1.5-d/r_{br}\sigma_{br})} \quad (11)$$

where q_{bca} is the transport capacity per unit width for sediment moving on purely alluvial bed and q_{bcb} is the transport capacity per unit width for sediment moving on purely bedrock bed. τ_{*cb} is the dimensionless critical shear stress for grains on bedrock portions of the bed.

https://doi.org/10.5194/esurf-2019-78
Preprint. Discussion started: 4 February 2020


Earth Surface Dynamics Discussions
Open Access
EGU

The two models may seem rather similar in that they estimate the transport capacity of a mixed alluvial – bedrock surface. However, both models opt for different approaches when it comes to estimating hydraulic roughness. The model by Inoue et al. (2014) directly uses the hydraulic roughness, but the model by Johnson (2014) calculates the hydraulic roughness from the topographic unevenness of the bed surface. In the model by Inoue et al. (2014), the topographic unevenness (i.e., macro roughness) acts only when converting the alluvial layer thickness to the alluvial cover ratio. The macro roughness affects the temporal change of the alluvial cover ratio, but does not affect the alluvial cover ratio in the dynamic equilibrium state. In addition, in the model by Johnson (2014), first, the sediment transport capacities for the bedrock and alluvial bed are separately calculated, then total transport capacity is estimated using P_c. However, in the model by Inoue et al. (2014), first the total hydraulic roughness height is calculated using P_c, then total transport capacity is estimated using the total hydraulic roughness. Turowski and Hodge (2017) proposed a probability based model for prediction of cover on bedrock channels. They proposed cover consisting of combined exponential and linear effects of sediment supply.

$$P_c = 1 - \left[1 + (1-\omega) ln\left\{1 - \left(1 - e^{-M_0^* q_{bs}}\right) q_{bs}\right\}\right] \quad (12)$$

where ω is the exponent, M_0^* is the dimensionless characteristic sediment mass obtained as following:

$$M_0^* = \frac{3\sqrt{3}\tau_{*c}}{2\pi} \frac{\tau_*/\tau_{*c} - 1}{(\tau_*/\tau_{*c})^{0.5} - 0.7} \quad (13)$$

M_0^* follows a linear relationship with τ_* for a high τ_*. They suggested that on shorter time scales, the sediment cover follows a linear relationship with the sediment supply, but on longer time scales the channel adjusts its slope and width.

We hereafter refer Sklar and Dietrich (2004) model as linear model, Turowski et al.'s model (2007) as exponential model, Inoue et al.'s model (2014) as macro roughness model, Meyer-Peter and Müller (MPM) based Johnson's model (2014) as surface roughness model and Turowski and Hodge's model (2017) as probabilistic model.

https://doi.org/10.5194/esurf-2019-78
Preprint. Discussion started: 4 February 2020

Earth Surface Dynamics Discussions
Open Access
EGU

2 Experimental Method

2.1 Experimental Flume

The experiments were conducted in a straight channel at the Civil Engineering Research Institute for Cold Region, Sapporo, Hokkaido, Japan. The experimental channel was 22m long, 0.5m wide and had a slope of 0.01. The width-depth ratio was chosen to achieve no-sandbar condition (i.e., small width-depth ratio, 6.1 to 8.3 in our experiments). Chatanantavet and Parker (2008) conducted several flume experiments with sandbar condition (i.e., large width-depth ratio, 11 to 30 in their experiments) and suggested that the alluvial cover increases linearly to the ratio of sediment supply and transport capacity of the channel when the slope is less than 0.015. In this study, we investigated the influence of bedrock roughness on the alluvial cover under conditions where the slope and width - depth ratio were small compared to the experiments of Chatanantavet and Parker (2008).

2.2 Bed characteristics and conditions

The channel bed consisted of non-erodible mortar. In order to achieve different roughness conditions, the beds in Run 1, Run 2 and Run 3 were embedded with gravel of different particle sizes. In Run 1, the embedded particle size is 30 mm, in Run 2 particle size of 50 mm is embedded and in Run 3, 5 mm particle size is embedded.

We performed an additional 2 cases with net-installation on the river bed. An installed net on the river bed can trap sediment during high flow, eventually protecting the bed from further erosion from abrading sediment (Kazuaki et al.,2015, in Japanese). A net of mesh size 30 mm X 30 mm was installed on the bed in Run 4 and Run 5. The height of the net was 4mm and 2 mm respectively. Figure 1 shows the experimental channel bed of all 5 runs.

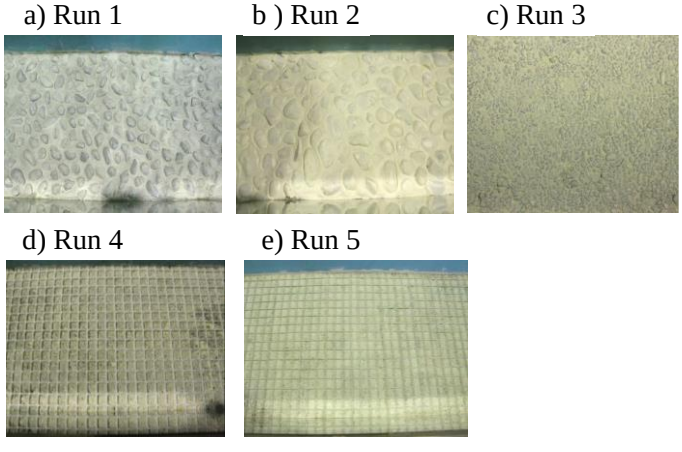

Figure 1: Initial channel bed for each run.

https://doi.org/10.5194/esurf-2019-78
Preprint. Discussion started: 4 February 2020


Earth Surface Dynamics Discussions Open Access EGU

2.3 Measurement of bedrock roughness

In order to measure the initial bed roughness (before supplying sand), a water discharge of 0.03 m^3/s was supplied, and the water level was measured longitudinally at every 1 m at the centre of the channel. Manning's coefficient was calculated using the water level.

$$n_m = \frac{1}{U} D^{2/3} {S_e}^{1/2} \quad (14)$$

where n_m is the Manning's roughness coefficient and U is the average velocity ($U = Q/wD$ where U is the water discharge, w is the channel width, D is the water depth), S_e is the energy gradient.

In order to compare the hydraulic roughness height and the riverbed-surface unevenness height, the riverbed height before water flow was measured with a laser sand gauge. The measurements were taken longitudinally at every 5 mm. The measurements were taken at three points: 0.15 m away from the right wall, the centre of the channel, and 0.15 m away from the left wall. The standard deviation representing the topographic roughness σ_{br} was obtained by subtracting the mean slope from the riverbed elevation (Johnson and Whipple; 2010).

2.4 Measurement of dimensionless critical shear stress on bedrock

In order to measure the dimensionless critical shear stress of grains on completely bedrock portion, i.e. τ_{*cb}, 30 gravels with diameter of 5mm were placed on the waterway floor at intervals of 10 cm or more to make sure that there was no shielding effect between the gravels (there was shielding effect due to unevenness of the bedrock). Next, water flow was supplied at a rate that no gravel moved, and was slowly increased to a rate at which all the gravels moved. The water level and the number of gravels displaced were measured and recorded for each flow rate.

The weighted average of the dimensionless shear stress $\tau_* = DS_e/Rd$ was obtained using the measured number of movement.

2.5 Validation of alluvial-cover

Different amounts of sand were supplied manually while the flow rate was kept constant at 0.03 m^3/s. The alluvial cover ratio was measured once equilibrium state was achieved. The sediment supply amounts and other experimental conditions for various cases are provided in Table 1. Each run has multiple cases, each with different sediment supply and time duration. Each case was performed unless the P_c became constant. The gravels were supplied from Run-0 of no sediment to Run-4~5 of completely alluvial cover. The Run-0 with no sediment supply in each run represents the bedrock-roughness measurement experiment explained in section 2.3.

Equilibrium conditions were achieved after 2-4 hours of sand supply. The alluvial cover was calculated from black and white photographs of the flume by taking the ratio of the number of pixels. The water level was measured and recorded every hour at the centre of the channel in order to calculate the hydraulic roughness during and at the end of the experiment.

https://doi.org/10.5194/esurf-2019-78
Preprint. Discussion started: 4 February 2020

Earth Surface Dynamics Discussions
Open Access
EGU

Table 1: Experimental Conditions

Run	k_{sb} (mm)	k_{sb}/d	q_{bs} ($\times 10^{-5}$m^2/s)	Time (hour)	P_c	D	U	Fr
Run1-0	48.0	9.6	0.00	0.25	0.00	0.082	0.74	0.82
Run1-1			0.93	4.00	0.55	0.082	0.73	0.82
Run1-2			1.87	4.00	0.75	0.082	0.74	0.82
Run1-3			2.80	4.00	0.93	0.082	0.74	0.82
Run1-4			3.73	4.00	0.99	0.082	0.73	0.82
Run2-0	24.8	5.0	0.00	0.25	0.00	0.078	0.83	0.95
Run2-1			0.93	4.00	0.20	0.077	0.79	0.91
Run2-2			1.87	4.00	0.34	0.077	0.79	0.91
Run2-3			2.80	4.00	0.46	0.074	0.82	0.97
Run2-4			3.73	5.00	0.91	0.075	0.80	0.93
Run3-0	3.8	0.8	0.00	0.25	0.00	0.063	0.95	1.21
Run3-1			3.73	2.00	0.01	0.063	0.95	1.20
Run3-2			5.60	2.00	0.03	0.060	1.00	1.30
Run3-3			7.47	4.00	1.00	0.063	0.96	1.23
Run4-0	36.3	7.3	0.00	0.25	0.00	0.077	0.78	0.90
Run4-1			0.93	4.00	0.46	0.079	0.76	0.87
Run4-2			1.87	4.00	0.62	0.079	0.76	0.87
Run4-3			2.80	4.00	0.81	0.079	0.76	0.86
Run4-4			3.73	5.00	0.99	0.078	0.77	0.89
Run5-0	9.6	1.9	0.00	0.25	0.00	0.068	0.88	1.08
Run5-1			3.73	4.00	0.06	0.068	0.88	1.08
Run5-2			4.67	6.00	1.00	0.068	0.88	1.07
Run5-3			5.60	4.00	1.00	0.068	0.88	1.07

https://doi.org/10.5194/esurf-2019-78
Preprint. Discussion started: 4 February 2020

Earth Surface Dynamics Discussions
Open Access
EGU

3 Experimental results

3.1 Initial topographic roughness and hydraulic roughness

Figure 2 shows the relationship between the hydraulic roughness height of bedrock bed k_{sb} and the topographic roughness height of bedrock bed σ_{br}. This figure suggests that Run 1 with 30 mm sized embedded gravel, has the largest hydraulic roughness and Run 3 with 5 mm sized embedded gravel has the lowest hydraulic roughness. Run 2 embedded with 50 mm gravel has large topographical roughness error bars for the reason that, the large gravels were embedded randomly in the bed, resulting in unintended spatial variation in the unevenness of the channel bed. Although the hydraulic roughness tends to increase with an increase in topographical roughness, it has large variation. This variation is due to the fact that the hydrological roughness height does not only depend on the topographical roughness but also on the arrangement of the unevenness.

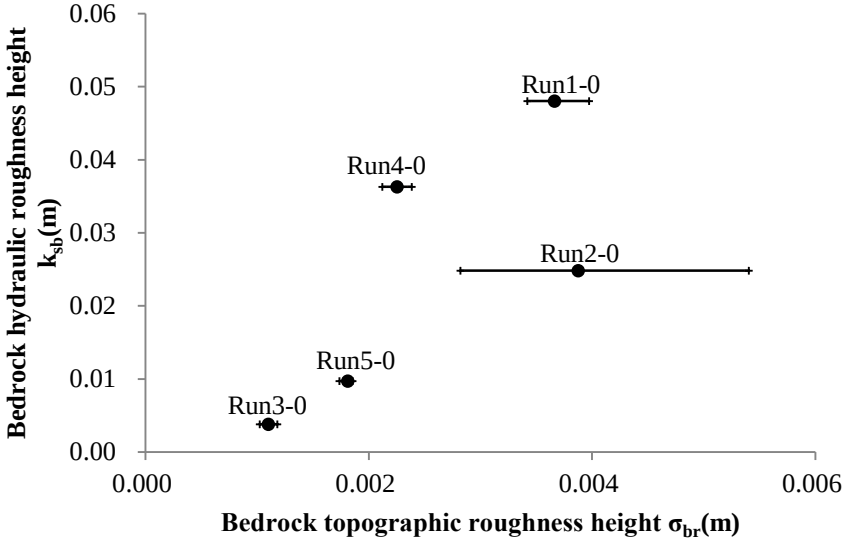

Figure 2: Relationship between initial bed hydraulic roughness height and topographic roughness height. The black circles in the image represent the average values measured on the three data collection lines, and the error bars represent the minimum and maximum value.

https://doi.org/10.5194/esurf-2019-78
Preprint. Discussion started: 4 February 2020

215 **3.2 Relative roughness, sediment supply and alluvial cover**

Figure 3 shows the channel bed after the experiments of the Run 1 series (Run 1-1, Run 1-2, Run 1-3 and Run 1-4) with the highest relative roughness. Figure 4 shows the channel bed after the experiments of the Run 3 series (Run 3-1, Run 3-2, Run 3-3) which has the lowest relative roughness. In these two figures, we can compare Run 1-4 and Run 3-1 with equal sediment supply rates. It can be seen that the bed in Run 1-4 is completely covered with sediment whereas the bed in Run 3-1 has almost
220 no accumulated sediment on the bed.

Figure 5 shows the relationship between alluvial-cover fraction Pc and sediment supply per unit width q_{bs}. P_c is obtained by dividing the sediment-covered area by the total area of the channel from photographs. The value of P_c is 1 for a completely covered channel and 0 for a completely exposed bedrock bed. In Figure 5, if we compare Run 1-4, Run 2-4, Run 3-1, Run 4-4 and Run 5-1, the cases with equal sediment supply rate of 3.73×10^{-5} m^2/s, it can be observed that alluvial-cover fraction is
225 increasing with an increase in the bedrock roughness. Moreover, in Run 1 series, Run 2 series and Run 4 series with high relative roughness k_{sb}/d (ratio of the hydraulic roughness height of bedrock bed k_{sb} to the grain size d), P_c is roughly proportional to the sediment supply rate q_{bs}. However, in Run 3 series and Run 5 series, which have lower k_{sb}/d (relative roughness), P_c shows hardly any increase when qbs is low (Run 3-0, Run 3-1, Run 3-2, Run 5-0, Run 5-1) and when sediment supply (q_{bs}) increases (Run 3-3, Run 5-2), the bedrock suddenly transitions to completely alluvial bed.

230

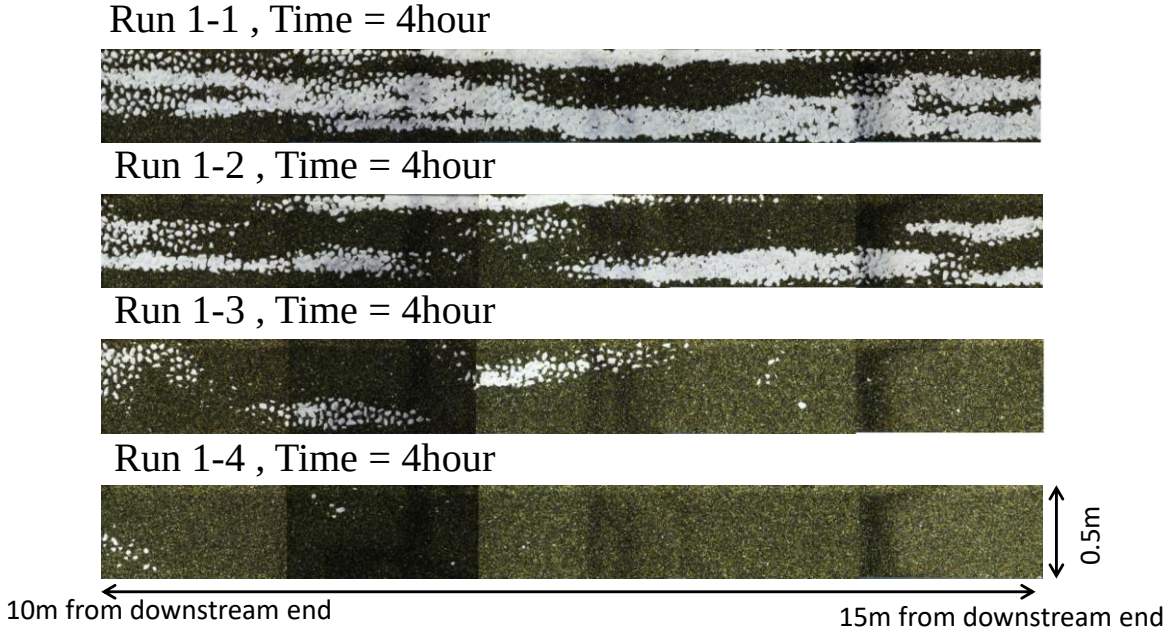

Figure 3: Bedrock exposure in Run 1 series at the end of the experiment. Initial bed had 30mm embedded particles.

https://doi.org/10.5194/esurf-2019-78
Preprint. Discussion started: 4 February 2020

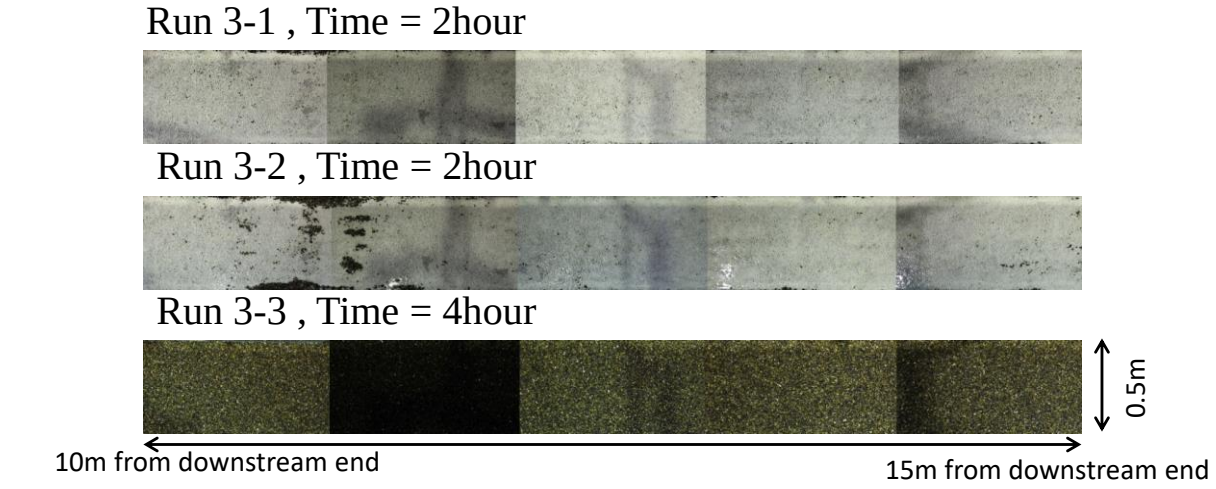

Figure 4: Bedrock exposure in Run 3 series at the end of the experiment. Initial bed had 5mm embedded particles.

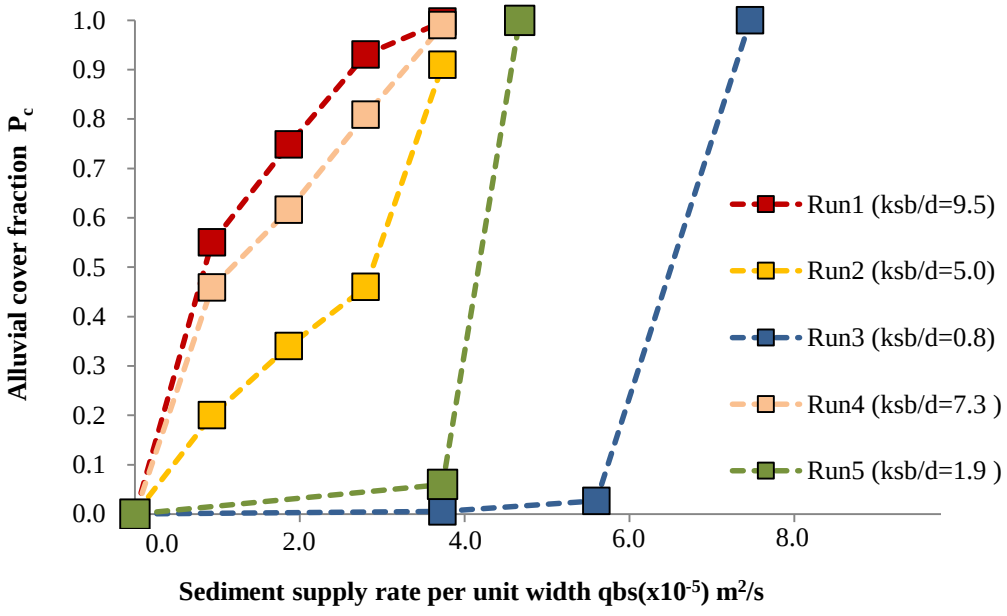

235

Figure 5: Variation in alluvial cover fraction (Pc) with sediment supply.

https://doi.org/10.5194/esurf-2019-78
Preprint. Discussion started: 4 February 2020

Earth Surface Dynamics Discussions
Open Access
EGU

3.3 Relationship between gravel layer thickness and alluvial cover fraction

Various studies have employed alluvial cover as a function of gravel bed thickness (Zhang et al., 2015; Inoue et al., 2014; Parker et al., 2013; Tanaka and Izumi, 2013 (in Japanese))

$$P_c = \begin{cases} \eta_a/L & for\ \ 0 \le \eta_a/L \le 1 \\ 1 & for\ \ \eta_a/L > 1 \end{cases} \quad (15)$$

here, η_a is the average thickness of the alluvial layer, L is the macro-roughness height of the bedrock bed. Parker et al. (2013) define L as the macroscopic asperity height of rough bedrock rivers L_b ($\fallingdotseq 2\sigma_{br}$). Tanaka and Izumi (2013) define L as the surface unevenness of alluvial deposits on smooth bedrock river L_a ($\fallingdotseq d$). In this study, we define L = $2\sigma_{br}$+d so that it can cope with both smooth and rough bedrocks. Figure 6 shows the relationship between relative gravel layer thickness ηa/L and alluvial cover ratio. The figure confirms that the alluvial cover ratio of the experimental result can be efficiently evaluated by Equation (15).

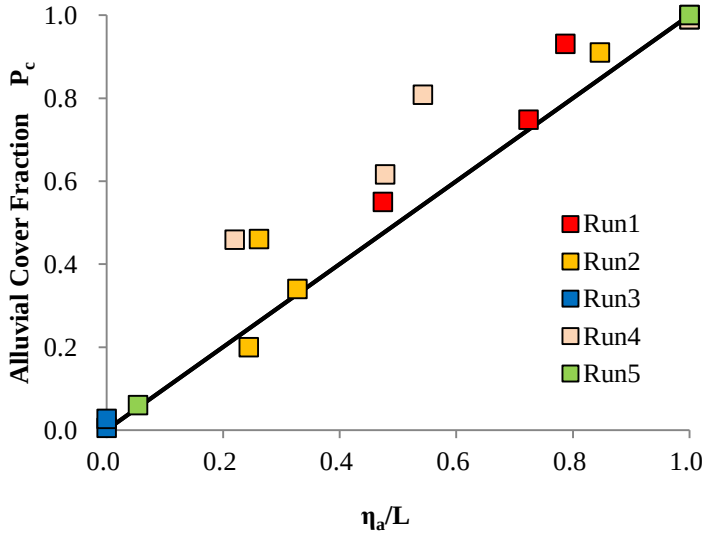

Figure 6: Relationship between relative gravel layer thickness and alluvial cover.

https://doi.org/10.5194/esurf-2019-78
Preprint. Discussion started: 4 February 2020

Earth Surface Dynamics Discussions
Open Access
EGU

3.4 Time series change of relative roughness

Figure 7 shows the change in relative roughness with time in Run 1 and Run 3 series. The red and blue points in Figure 7 show the alluvial cover fraction after water supply in Run 1 and Run 3 series respectively.

In Run 1 series with a higher relative roughness, it can be seen that relative roughness decreased due to the increase in alluvial deposition and cover. In Run 3 series which has a lower initial relative roughness increased due to the increase in alluvial deposition and cover.

The relative roughness after the water supply is ~2 for both Run1-4 and Run3-3 while the alluvial cover fraction approaches 1. This value is almost the same as the relative roughness of flat gravel bed (about 1 to 4 times the particle size, generally about 2 times). This confirms that with an increase in alluvial cover, the relative roughness of the bed is determined by the gravel size.

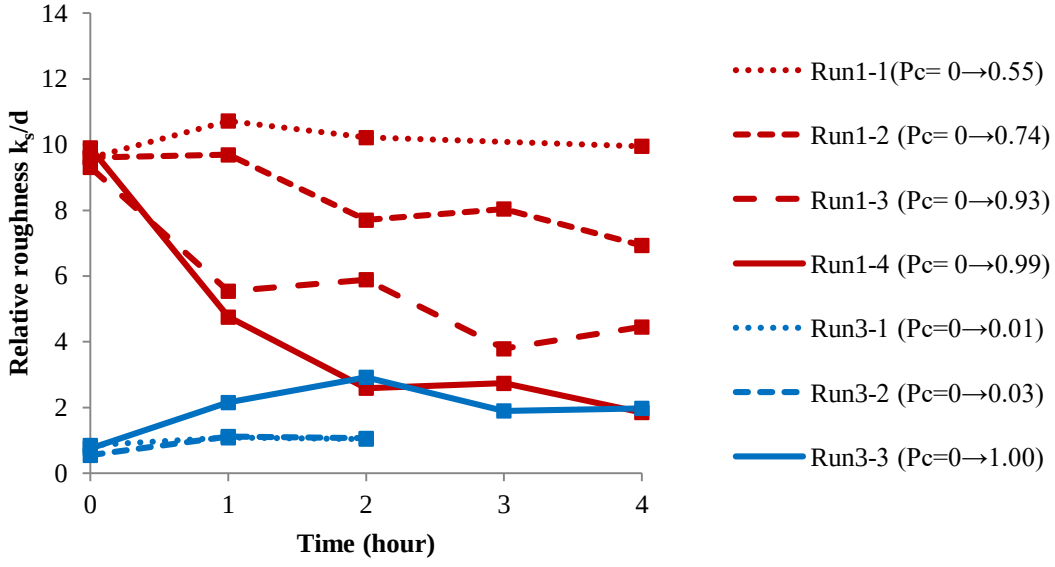

Figure 7: Change in Relative roughness with time.

https://doi.org/10.5194/esurf-2019-78
Preprint. Discussion started: 4 February 2020

Earth Surface Dynamics Discussions
Open Access
EGU

4 Discussion and Comparison of the Existing Models with Experimental Results

4.1 Relative Roughness and dimensionless critical shear stress

Figure 8 shows the relationship between the ratio of the hydraulic roughness height of bedrock bed k_{sb} to the grain size d (k_{sb}/d: referred to as the relative roughness in section 3.2) and the dimensionless critical shear stress over bedrock bed τ_{*cb}. The Figure shows results obtained from Johnson (2014) (Eq. 10) and from Inoue et al. (2014) (Eq. 5) i.e. surface-roughness model and macro-roughness model respectively.

According to Figure 8, the non-dimensional critical shear stress depends on the relative roughness to the power of 0.6. Besides, the results obtained from Eq. (5) of macro-roughness model are not compatible with the experimental results in the region where relative roughness of the bedrock bed is small. In this study, we used the power approximation shown below instead of Eq. (5) in the macro roughness model by Inoue et al. (2014).

$$\tau_{*c} = 0.03(k_s/d)^{0.6} \quad (15)$$

Likewise, the results obtained from Johnson's model (2014) (Eq. 10) (surface-roughness model) are consistent with our experimental results, but the model is inconsistent when the roughness is low.

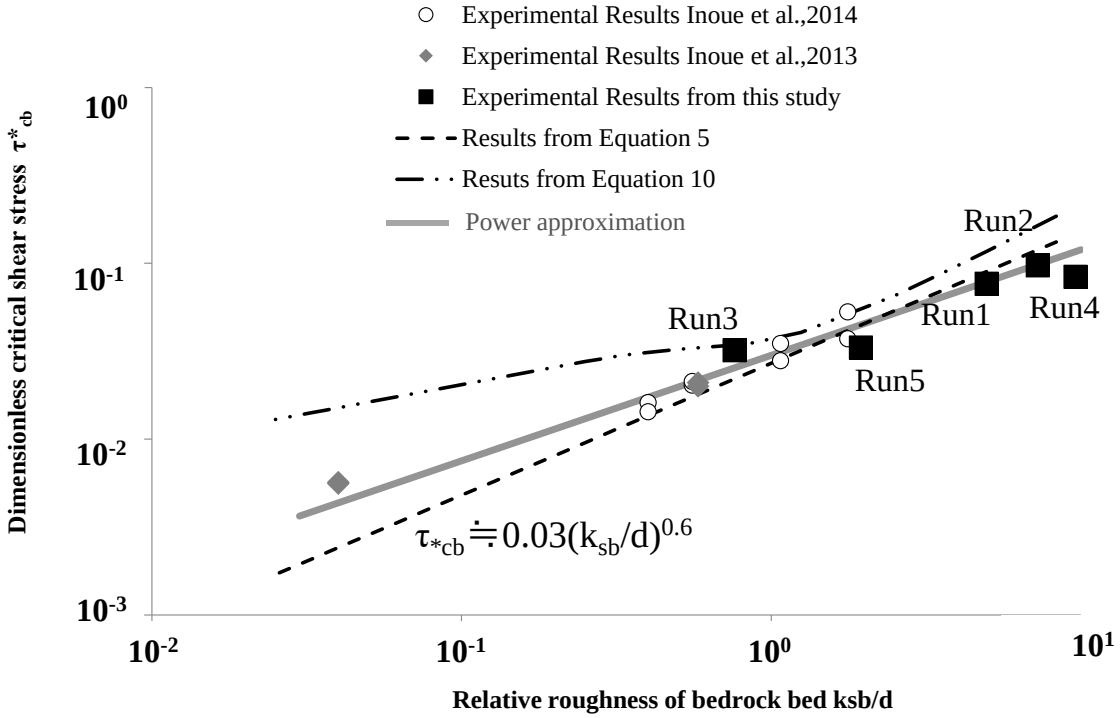

Figure 8: Relationship between relative roughness and dimensionless critical shear stress. The black squares show the results of this experiment, the white circles show the results of investigation using the bedrock of Ishikari River in 2011 (Inoue et al., 2014), the grey rhombus represents a smooth aquifer floor (Inoue and Ito, 2013 (in Japanese)), the grey line shows the power approximation of all the experimental results. The dotted line shows the results from Eq. 5 proposed by Inoue et al. (2014). The black double dotted lines show the results obtained by Eq. 10 (Johnson, 2014).

https://doi.org/10.5194/esurf-2019-78
Preprint. Discussion started: 4 February 2020

Earth Surface Dynamics Discussions
Open Access
EGU

4.2 Calibrating $k_{\#D}$ and r_{br}

For the purpose of model comparisons with experimental results, we need to first calibrate Johnson's model parameters $k_{\#D}$ and rbr to minimize RMSD (root mean square deviation). When $k_{\#D} = 1$, it means the alluvial hydraulic roughness is proportional to the grain diameter size and is independent of the cover fraction. For our calculations, we have used $k_{\#D} = 4$ as applied in Johnson (2014). We also calibrate the exponential model's parameter φ (Turowski et al, 2007). Table 2 provides the calibration values for r_{br} and φ for comparison of the model with our experimental results.

Table 2: r_{br} and φ values for comparison with experimental results

	Observed k_{sb} (mm)	Observed σ_{br} (mm)	Adjusted r_{br} ($k_{\#D}$=4)	Calculated k_{sb} (mm, $k_{sb}=r_d\, r_{br}\sigma_{br}$)	Adjusted φ
Run 1	48.0	3.7	3.0	22.2	3.1
Run 2	24.8	3.9	2.1	16.4	1.1
Run 3	3.8	1.1	3.0	6.6	0.4
Run 4	36.3	2.3	4.6	21.2	2.2
Run 5	9.6	1.8	2.6	9.4	0.9

4.3 Predicting experimental results using the models

Figure 9 shows the comparison among experimental results presented in this paper, Sklar and Dietrich's linear model (2014), Turowski et al.'s exponential model (2007), Inoue et al.'s macro-roughness model (2014) and Johnson's surface-roughness model (2014) This Figure suggests that the linear model is generally applicable to rough bed with relative roughness of 2 or more, but not to "smoother bed" with relative roughness less than 2 (Run 1, Run 2 and Run 4). As suggested by Inoue et al. (2014), in this study, "smooth bed" refers to the bed with roughness less than the roughness of supplied gravel and "rough bed" stands for the bed with roughness more that the roughness of the supplied gravel. The exponential model is also more suitable for a rough bed. The figure also shows that the macro-roughness model proposed by Inoue et al. (2014) can predict the increasing alluvial cover for cases with high relative roughness, as well as the runaway hysteresis for cases with lower relative roughness (Run 3 and Run 5), without adjusting the roughness. The surface-roughness model proposed by Johnson (2014) also shows good agreement in predictions of alluvial cover and runaway hysteresis if $k_{\#D}$ and r_{br} are adjusted.

In Run 3 and Run 5 with relatively smooth beds, a rather scarce deposition was observed when sediment supply was low, and runaway alluviation occurred when sediment supply exceeded the transport capacity of the channel i.e. the bed was suddenly completely covered by alluvium. The reverse-line slopes produced by macro-roughness and surface-roughness models depict similar hysteresis relationship between alluvial cover and sediment supply i.e. sediment deposition occurs only for a certain range of sediment supply. This phenomenon has also been observed in sufficiently steep channels, for slopes greater than 0.015

https://doi.org/10.5194/esurf-2019-78
Preprint. Discussion started: 4 February 2020

by Chatanantavet and Parker (2008). Hodge and Hoey (2016b) also suggested a similar relationship between sediment cover and sediment supply. However, our study shows that rapid alluviation occurs irrespective of the slope steepness, if roughness of the bed is less than the roughness of supplied gravel, i.e. when relative roughness is less than 2.

In an effort to get a better understanding of the effectiveness of the two models: the macro-roughness model proposed by Inoue et al. (2014) and the surface-roughness model proposed by Johnson (2014)), we also compared the model results with experimental results of Chatanantavet and Parker (2008). They conducted experiments in a metallic straight channel with three different types of bedrock bed surfaces namely Longitudinal Grooves (LG), Random Abrasion Type 1 (RA1) and Random Abrasion Type 2 (RA2), where RA1 is smoother than RA2. They performed various cases for each type with varying slope range of 0.0115 – 0.03. They also varied the sediment supply rate and grain size (2mm and 7mm). The major difference between their experiment and our experiments is the width – depth ratio. The width-depth ratios of their experiments were 11 – 30, and thus allowed for the formation of alternate bars. In contrast, the width – depth ratios of our experiments were 6.1 – 8.3, as a result alternate bars usually do not develop. Although we can see alternate alluvial patches in Figure 5, their thickness was less than 1 cm, and the patches did not progress to alternate bars with large wave height. Figure 11 shows the comparison among the two models and Chatanantavet and Parker's experiment (2008). The experimental conditions are taken from Table 1 of Chatanantavet and Parker (2008). Figure 11a represents runs 2-C1 to 2-C4, Figure 10b represents runs 2-E1 to 2-E3, Figure 11c represents runs 3-A1 to 3-A5, Figure 11d represents runs 3-B1 to 3-B5, Figure 11e represents runs 1-B1 to 1-B4 (Chatanantavet and Parker 2008, Table 1). In case of the surface-roughness model, $k_{\#D} = 4$ is used, the bedrock surface roughness required for calculations is taken as mentioned in Table 1 Johnson (2014), r_{br} is adjusted to minimize RMSD. In case of the macro-roughness model by Inoue et al. (2014), k_{sb} is adjusted to minimize RMSD. The two models can accurately predict the cover fraction and runaway alluviation for the experimental study conducted by Chatanantavet and Parker (2008). A very important point of interest is the adjustment of hydraulic roughness value of the bedrock surface k_{sb}. In case of Chatanantavet and Parker's experiment, k_{sb} ~ 0.4 mm to 3.5mm (Chatanantavet and Parker 2008, Table 1), whereas, in Johnson's surface-roughness model (2014), k_{sb} $(= r_d r_{br} \sigma_{br})$ can be as much as 13 – 27 mm. Also, in the case of Inoue et al.'s macro-roughness model k_{sb} is adjusted to 32 – 53 mm (Table 3).

Figure 10 shows the comparison of experimental results with Turowski and Hodge's probabilistic model (2017). The model produces favourable results following some parameter adjustments. The values of exponent ω and characteristic sediment mass M_0^* needs to be adjusted by trial and error. The value of ω can be as high as 100 or 200 for Runs with runaway hysteresis, whereas it is as low as ~0.7 for other Runs.

https://doi.org/10.5194/esurf-2019-78
Preprint. Discussion started: 4 February 2020

Table 3: Parameter calibration values for comparison with experimental results of Chatanantavet and Parker (2008)

Type	Slope	Observed k_{sb} (mm)	σ_{br} (mm)	Adjusted r_{br} for the surface-roughness model $k_{\#D}$=4	Calculated k_{sb} in the surface-roughness model (mm, $k_{sb}= r_d\, r_{br}\sigma_{br}$)	Adjusted k_{sb} for the macro-roughness model (mm)
LG	0.02	0.4	6.7	1.8	24.1	42.0
RA1	0.016	0.4	2.4	5.3	25.4	42.0
	0.03	0.4	2.4	5.7	27.4	53.0
RA2	0.0115	3.5	2.7	2.5	13.5	32.0
	0.02	3.5	2.7	4.3	23.2	45.0

4.4 Differences and limitations

As mentioned earlier, the major difference between the two models employed in this study is the way the transport capacity is calculated. In case of the surface-roughness model (Johnson, 2014), first, the transport capacities for bedrock (q_{bcb}) and alluvial bed (q_{bca}) are separately calculated, then the total transport capacity (q_{bc}) is calculated for a range of cover fractions (P_c). Hence, in cases when $\tau_{*c} < \tau_* < \tau_{*cb}$, the transport capacity over bedrock portion $q_{bcb} = 0$. As a result, bedrock roughness is hardly affected by the alluvial cover fraction which can also be the reason for inconsistency between the surface-roughness model results and experimental study for Runs 1 and 4 in Figure 9 and RA2 Slope = 0.0115 in Figure 11. Whereas, in the case of macro-roughness model (Inoue et al., 2014), the critical shear stress takes into account the value of total hydraulic roughness, which depends on cover fraction, alluvial hydraulic roughness and bedrock hydraulic roughness. Hence, even when τ_* is small, the bedrock roughness tends to affect the cover fraction.

Comparing the observed k_{sb} with the adjusted k_{sb} in the roughness models proposed by Inoue et al. (2014) and Johnson (2014), the adjusted k_{sb} strongly depends on observed k_{sb} in our experiments without alternate bars (Figure 12a), whereas, the adjusted k_{sb} is not dependent on the observed k_{sb} in experiments with alternate bars conducted by Chatanantavet and Parker (2008) (Figure 12b), suggests that bedrock roughness has a smaller effect on the alluvial cover in case of mixed alluvial – bedrock rivers with alternate bars. In such rivers, the bed slope may affect the alluvial cover fraction (Figure 12c). The roughness models are adjusted to produce the experimental results with alternate bars by fine-tuning r_{br} and k_{sb} values which have to be determined by trial and error method. While this method can be applicable to laboratory-scale experiments, the model calibration is unfeasible for a large-scale channel or natural rivers. In general, the formation of alternate bars is barely reproduced with a one-dimensional model as introduced in this study. In the future, research to incorporate the effects of bars into a one-dimensional model, or analysis using a two-dimensional planar model (e.g., Nelson and Seminara, 2012; Inoue et al., 2016, 2017) is expected.

https://doi.org/10.5194/esurf-2019-78
Preprint. Discussion started: 4 February 2020

Earth Surface Dynamics Discussions
Open Access
EGU

Also, the probabilistic model proposed by Turowski and Hodge (2017) could reproduce experimental results but the model needed adjustment of ω and M_0^* by trial and error, specially for cases involving runaway hysteresis.

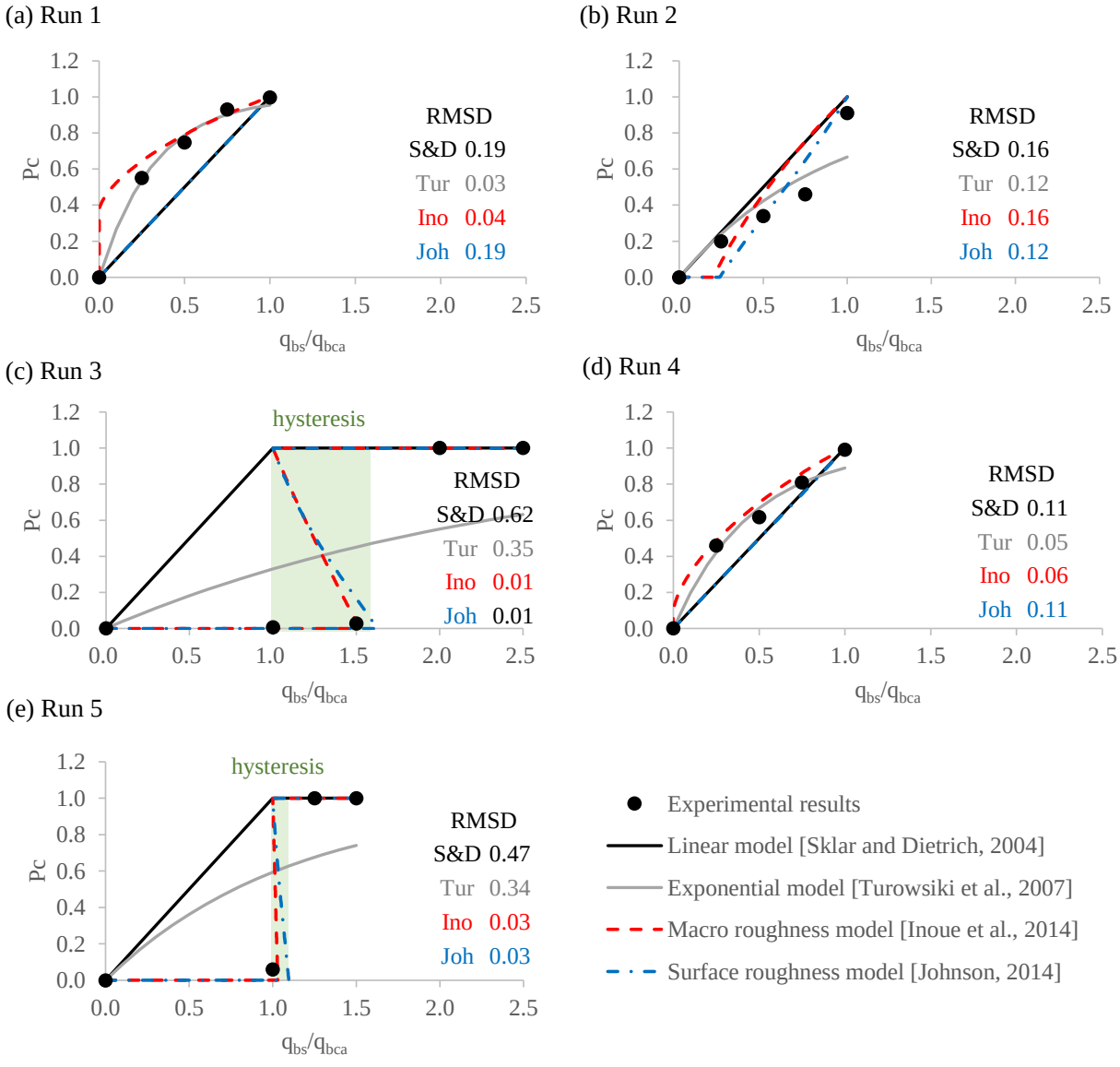

Figure 9: Comparison of experimental results, linear model by Sklar and Dietrich (2004), exponential model by Turowski et al. (2007), roughness models by Inoue et al. (2014) and Johnson (2014). The r_{br} for the surface roughness model and the φ for the exponential model are adjusted to minimize RMSD.

https://doi.org/10.5194/esurf-2019-78
Preprint. Discussion started: 4 February 2020

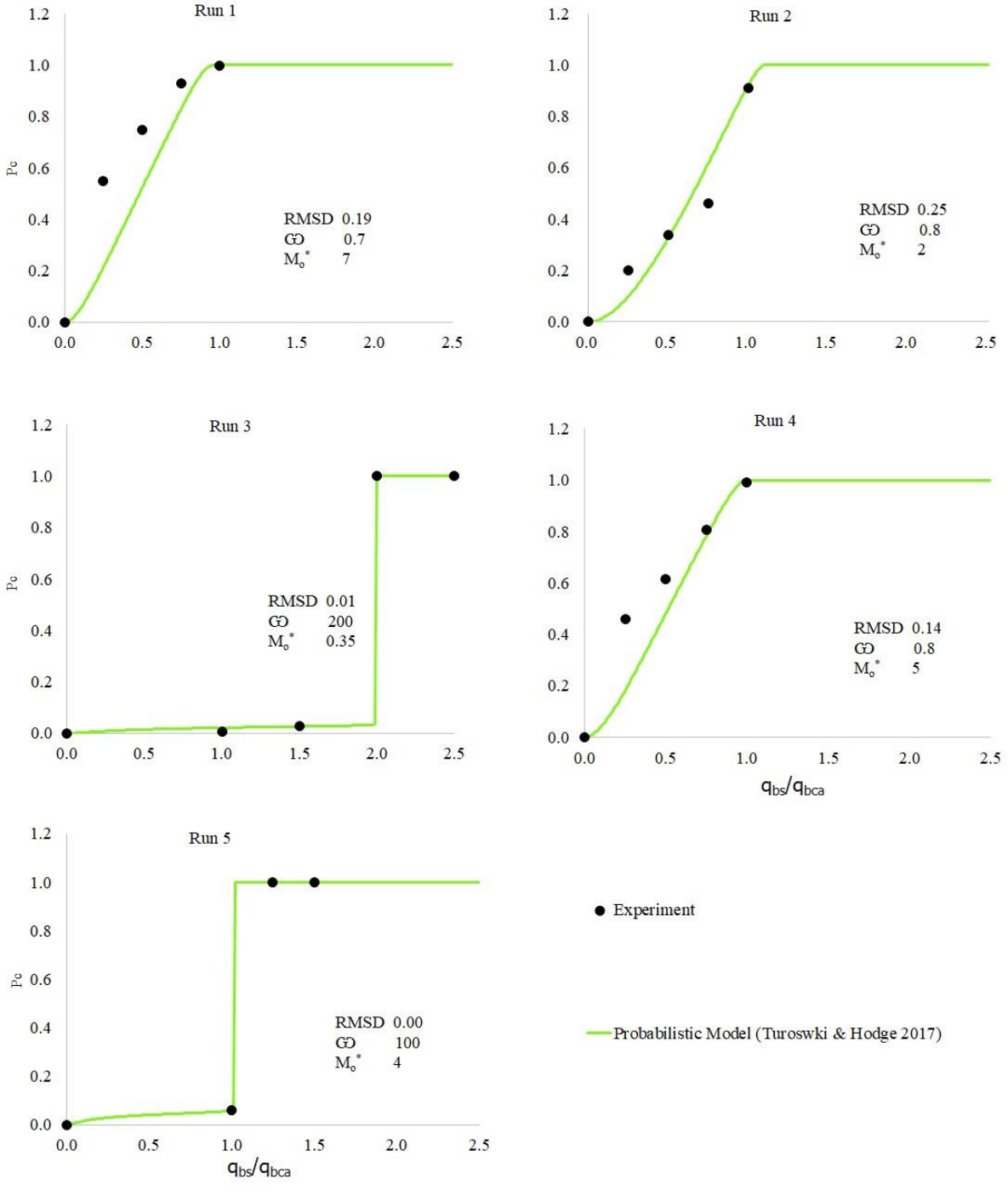

Figure 10: Comparison of Experimental results with Turowski and Hodge's probabilistic model (2017).

https://doi.org/10.5194/esurf-2019-78
Preprint. Discussion started: 4 February 2020

Earth Surface Dynamics Discussions
Open Access
EGU

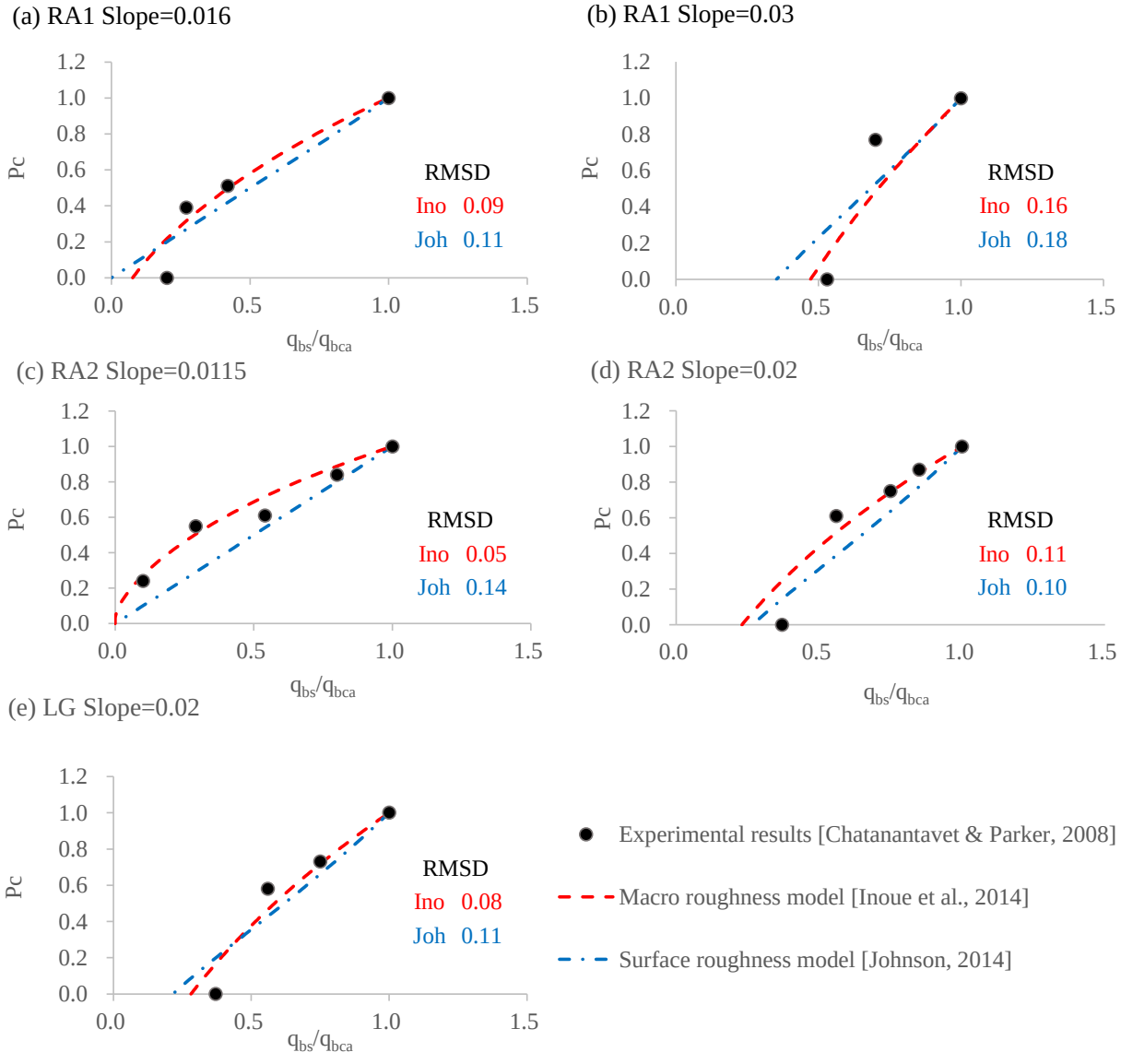

Figure 11: Comparison of the experimental results (Chatanantavet and Parker, 2008) with the macro roughness model (Inoue et al., 2014) and the surface roughness model (Johnson, 2014). RA1 in (a) and (b) represent Random Abrasion type 1, RA2 in (c) and (d) represent Random Abrasion type 2, LG in (e) represents Longitudinal grooves (Chatanantavet and Parker 2008). The r_{br} for the surface roughness model and the k_{sb} for macro roughness model are adjusted to minimize RMSD.

https://doi.org/10.5194/esurf-2019-78
Preprint. Discussion started: 4 February 2020

Earth Surface Dynamics Discussions
Open Access
EGU

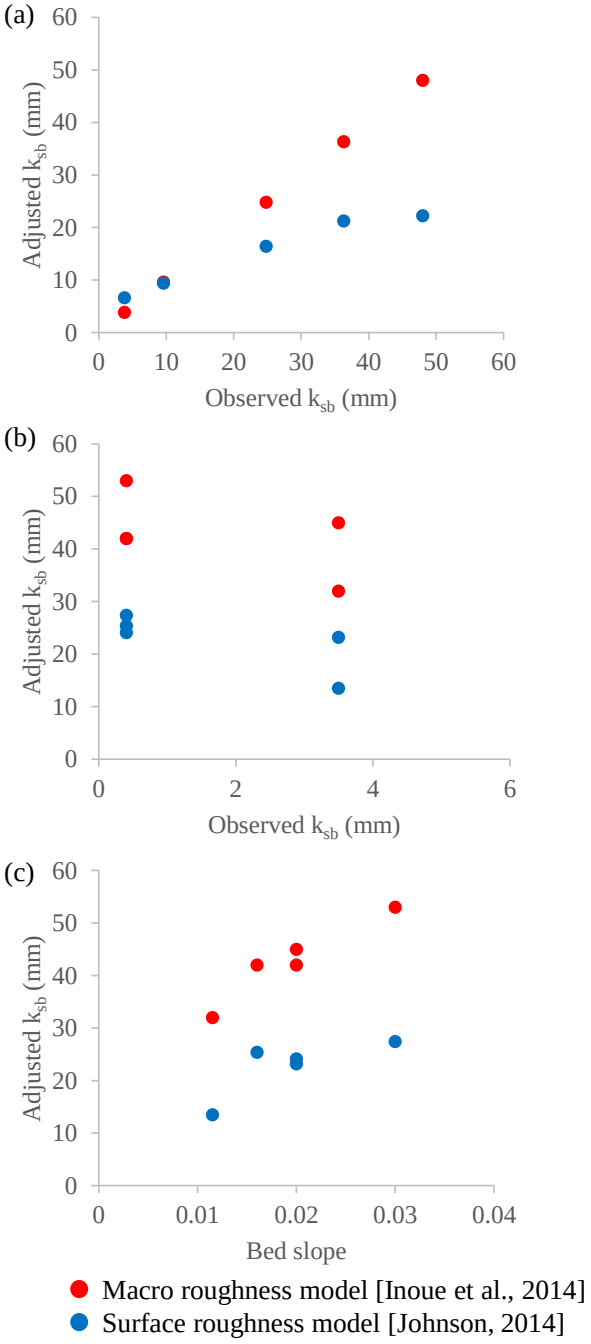

380 **Figure 12: (a) Comparison between adjusted hydraulic roughness height of bedrock bed k_{sb} and observed k_{sb} for experiments conducted in this study by us. (b) Comparison between adjustedk_{sb} and observed k_{sb} for Chatanantavet and Parker's experiment (2008). (c) Sensitivity of adjusted k_{sb} to bed-slope S for experiments conducted by Chatanantavet and Parker (2008).**

https://doi.org/10.5194/esurf-2019-78
Preprint. Discussion started: 4 February 2020

5 Summary

Here we provide a review of models and studies focused at discovering the interaction between alluvial cover and bed roughness. In order to get an insight into the interaction between alluvial cover and bed roughness, we conducted laboratory-scale experiments with multiple runs of varying bed roughness and sediment supply. The experimental results show that the change in alluvial cover to the supplied sediment is controlled by bed roughness to a great extent. When the bedrock hydraulic roughness is higher than the hydraulic roughness of the alluvial bed, the alluvial cover increases proportionately with the increase in sediment supply and then reaches an equilibrium state. However, in cases where bedrock roughness is lower than the roughness of the alluvial bed, i.e. the bed is smoother than the sediment supplied, the deposition is insignificant unless sediment supply exceeds the transport capacity of the channel, after which, the bed abruptly becomes completely alluvial.

We have also implemented the cover-roughness interaction models: the linear model proposed by Sklar and Dietrich (2004), the exponential model by Turowski et al. (2007), the macro-roughness model by Inoue et al. (2014) , the surface-roughness model by Johnson (2014) and the probabilistic model by Turowski and Hodge (2017) in order to predict the experimental results. The linear model and exponential model are inefficient for cases with a smooth-bed specifically, they cannot predict the hysteresis. The macro-roughness model (Inoue et al. 2014) and surface-roughness model (Johnson, 2014) can efficiently predict the runaway-alluviation for smooth-beds as well as the proportionate increase in alluvial cover for rough-bed. In particular, the macro-roughness model (Inoue et al. 2014) was able to reproduce the observed alluvial cover ratio without adjusting the parameters. The probabilistic model by Turowski and Hodge (2017) could also reproduce the laboratory experiments but for cases with runaway hysteresis, the model parameters had to be adjusted.

We also tested the macro-roughness model (Inoue et al. 2014) and surface-roughness model (Johnson, 2014) for their capability to predict the experimental results observed by Chatanantavet and Parker (2008), in which the bedrock surface has alluvial alternate bar formations. Both models were able to reproduce the alluvial cover fraction ensuing significant parameter adjustments. The two models do not include the 2-D effects caused by variable alluvial deposition and formation of bars on bedrock. Building a physical model that can predict alluvial cover fraction with bar formation represents an exciting challenge in the future.

Author Contribution: *Authors have contributed equally towards the conceptualisation, writing, and conducting experiments for this manuscript.

Acknowledgements: Data used in this publication is available in this paper itself or available in the papers referred (Chatanantavet and Parker, 2008 and Johnson 2014). In proceeding with this research, we received valuable comments from Professor Yasuyuki Shimizu, Professor Norihiro Izumi, and Professor Gary Parker. We would like to express our gratitude here. The authors would also like to thank Jens M Turowski for his feedback that helped improve this paper.

https://doi.org/10.5194/esurf-2019-78
Preprint. Discussion started: 4 February 2020

Notations:

b_r	exposure function by Johnson (2014)
d	particle size (m)
D	water depth (m)
k_s	hydraulic roughness height (m)
k_{sa}	hydraulic roughness height of purely alluvial bed (m)
k_{sb}	hydraulic roughness height of purely bedrock bed (m)
$k_{\#D}$	non-dimensional alluvial roughness
l	flume length
L	macro-roughness height of bedrock bed (m)
N	number of spherical grain
M_0^*	dimensionless sediment mass
n_m	Manning's roughness coefficient
P_c	mean areal fraction of alluvial cover
q_{bs}	sediment supply rate per unit width (m^2/s)
q_{bc}	transport capacity per unit width (m^2/s)
q_{bca}	transport capacity per unit width for sediment moving on purely alluvial bed (m^2/s)
q_{bcb}	transport capacity per unit width for sediment moving on purely bedrock bed (m^2/s)
Q	water discharge (m^3/s)
r_d	scaling coefficient for *d* and hydraulic roughness length
r_{br}	fitting parameter that scales bedrock roughness to *d*
R	specific gravity of sediment in water (1.68)
S	Bed slope
S_e	energy gradient
U	depth averaged velocity (m/s)
w	flume width
α	bedload transport coefficient
η_a	average thickness of alluvial layer
κ	Karman constant
σ_{br}	topographic roughness height of purely bedrock bed (m)

https://doi.org/10.5194/esurf-2019-78
Preprint. Discussion started: 4 February 2020

τ_*	dimensionless shear stress
τ_{*c}	dimensionless critical shear stress
τ_{*ca}	dimensionless critical shear stress for grains on purely alluvial bed
τ_{*cb}	dimensionless critical shear stress for grains on purely bedrock bed
φ	cover factor proposed by Turowski et al. (2007)
ω	Exponent by Turowski and Hodge (2017)

https://doi.org/10.5194/esurf-2019-78
Preprint. Discussion started: 4 February 2020

References

Aubert, G., Langlois, V. J., and Allemand, P.: Bedrock incision by bedload: insights from direct numerical simulations, Earth Surf. Dynam.,4, 327–342, https://doi.org/10.5194/esurf-4-327-2016, 2016.

Byerlee, J.D.: Friction of rocks, Pure and Applied Geophysics 116 (4–5), 615–626,1978.

Chatanantavet, P., and Parker G.: Experimental study of bedrock channel alluviation under varied sediment supply and hydraulic conditions, Water Resour. Res., 44, W12446, doi:10.1029/2007WR006581, 2008.

Chepil, W. S.: The Use of Evenly Spaced Hemispheres to Evaluate Aerodynamic Forces on a Soil Surface, Transactions A.G.U., 39(3), 397-404, 1958.

Cowie, P. A., Whittaker A. C., Attal M., Roberts G., Tucker G. E., and Ganas A.: New constraints on sediment-flux-dependent river incision: Implications for extracting tectonic signals from river profiles, Geology, 36(7), 535–538, doi:10.1130/g24681a.1., 2008.

Egiazaroff, I. V.: Calculation of non-uniform sediment concentrations, J. Hydraul. Div. Am. Soc. Civ. Eng., 91, 225–247. 1965.

Finnegan, N. J., Sklar, L. S., & Fuller, T. K.: Interplay of sediment supply, river incision, and channel morphology revealed by the transient evolution of an experimental bedrock channel, Journal of Geophysical Research, 112, F03S11. https://doi.org/10.1029/2006JF000569, 2007.

Gilbert, G. K.: Report on the Geology of the Henry Mountains: Geographical and Geological Survey of the Rocky Mountain Region, , U.S. Gov. Print. Off., Washington, D. C., 160, doi:10.5962/bhl.title.51652, 1877.

Hodge, R. A., and Hoey, T. B. Upscaling from grain-scale processes to alluviation in bedrock channels using a cellular automaton model, J. Geophys. Res., 117, F01017, doi:10.1029/2011JF002145, 2012.

Hodge, R. A., and Hoey T. B.: A Froude-scaled model of a bedrock-alluvial channel reach: 1. Hydraulics, J. Geophys. Res. Earth Surf., 121, 1578–1596, doi:10.1002/2015JF003706, 2016a.

Hodge, R. A., and Hoey T. B.: A Froude-scaled model of a bedrock alluvial channel reach: 2. Sediment cover, J. Geophys. Res. Earth Surf., 121, 1597–1618, doi:10.1002/2015JF003709, 2016b.

Hodge, R. A., Hoey, T. B., and Sklar, L. S.: Bed load transport in bedrock rivers: The role of sediment cover in grain entrainment, translation, and deposition, J. Geophys. Res., 116, F04028, doi:10.1029/2011JF002032, 2011.

Inoue, T., and Ito A.: The relationship between roughness, critical Shear stress and sediment transport capacity on soft bedrock surface, Proceedings of the 68th Annual Conference of the Japan Society of Civil Engineers, II-072, 2013.

Inoue T.; Iwasaki T.; Parker G., Shimizu Y., Izumi N., Stark C. P., and Funaki J.: Numerical Simulation of Effects of Sediment Supply on Bedrock Channel Morphology. Journal of Hydraulic Engineering,142(7), 04016014- 1-11, doi:10.1061/(asce)hy.1943-7900.0001124, 2016.

https://doi.org/10.5194/esurf-2019-78
Preprint. Discussion started: 4 February 2020

Inoue, T., Izumi, N., Shimizu, Y., & Parker, G.: Interaction among alluvial cover, bed roughness, and incision rate in purely bedrock and alluvial-bedrock channel. Journal of Geophysical Research: Earth Surface, 119, 2123–2146. https://doi.org/10.1002/2014JF003133, 2014.

Inoue, T., Parker, G., and Stark, C. P.: Morphodynamics of a bedrock-alluvial meander bend that incises as it migrates outward: approximate solution of permanent form. Earth Surf. Process. Landforms, 42, 1342– 1354, doi:10.1002/esp.4094., 2017.

Johnson, J. P. L.: A surface roughness model for predicting alluvial cover and bed load transport rate in bedrock channels, J. Geophys. Res., 119, 2147–2173, https://doi.org/10.1002/2013JF003000, 2014

Johnson, J. P. L., and Whipple K. X.: Evaluating the controls of shear stress, sediment supply, alluvial cover, and channel morphology on experimental bedrock incision rate, J. Geophys. Res., 115, F02018, doi:10.1029/2009JF001335, 2010.

Johnson, J. P. L., Whipple K. X., Sklar L. S., and Hanks T. C.: Transport slopes, sediment cover, and bedrock channel incision in the Henry Mountains, Utah, J. Geophys. Res., 114, F02014, doi:10.1029/2007JF000862, 2009.

Johnson, J. P. L., Whipple, K. X., and Sklar, L. S.: Contrasting bedrock incision rates from snowmelt and flash floods in the Henry Mountains, Utah, Geological Society of America Bulletin,122(9–10), 1600–1615. https://doi.org/10.1130/b30126.1, 2010.

Kazuaki M., Inoue T., Shimizu Y.: Suppression method of soft rock erosion by using "net cover effect" and verification in real river, Advances in River Engineering, Vol.21, 165-170, 2015.

Meyer-Peter, E., and Müller R.: Formulas for bed-load transport, in Proceedings, Second Congress, International Association for Hydraulic Structures Research, Stockholm, 39–64, 1948.

Mishra, J., Inoue, T., Shimizu, Y., Sumner, T., & Nelson, J. M.: Consequences of abrading bed load on vertical and lateral bedrock erosion in a curved experimental channel, Journal of Geophysical Research: Earth Surf., 123, 3147– 3161. https://doi.org/10.1029/2017JF004387, 2018.

Nelson, P. A., and Seminara G.: A theoretical framework for the morphodynamics of bedrock channels, Geophys. Res. Lett., 39, L06408, doi:10.1029/2011GL050806, 2012.

Parker, G., Fernández, R., Viparelli, E., Stark, C. P., Zhang, L., Fu, X., Inoue, T., Izumi, N., and Shimizu, Y.: Interaction between waves of alluviation and incision in mixed bedrock-slluvial rivers, Advances in River Sediment Research, Proc. of 12th International Symposium on River Sedimentation, ISRS, 615-622, 2013.

Sklar, L. S., and Dietrich W. E.: River longitudinal profiles and bedrock incision models: Stream power and the influence of sediment supply, in Rivers Over Rock: Fluvial Processes in Bedrock Channels, Geophys. Monogr. Ser., vol. 107, edited by K. Tinkler and E. E. Wohl, pp. 237–260, AGU, Washington, D. C., doi:10.1029/GM107p0237, 1998.

Sklar, L. S., and Dietrich, W. E.: A mechanistic model for river incision into bedrock by saltating laboratory-scale, Water Resour. Res., 40, W06301, 2004.

Tanaka, G., and Izumi N.: The Bedload Transport Rate and Hydraulic Resistance in Bedrock Channels Partly Covered with Gravel, Journal of the Japan Society of Civil Engineers B1 (Hydraulic Engineering), Vol. 69, No. 4, I_1033-I_1038, 2013.

https://doi.org/10.5194/esurf-2019-78
Preprint. Discussion started: 4 February 2020

Turowski, J. M.: Stochastic modeling of the cover effect and bedrock erosion, Water Resour. Res., 45, W03422, doi:10.1029/2008WR007262, 2009.

Turowski, J. M. and Hodge, R.: A probabilistic framework for the cover effect in bedrock erosion, Earth Surf. Dynam., 5, 311–330, https://doi.org/10.5194/esurf-5-311-2017, 2017.

Turowski, J. M., Lague D., and Hovius N.: Cover effect in bedrock abrasion: A new derivation and its implications for the modeling of bedrock channel morphology, J. Geophys. Res., 112, F04006, doi:10.1029/2006JF000697, 2007.

Wilcock, P. R., and Crowe J. C.: Surface-based transport model for mixed-size sediment, J. Hydraul. Eng. Asce, 129(2), 120–128, doi:10.1061/(asce)0733-9429(2003)129:2(120), 2003.

Yanites, B. J., Tucker G. E., Hsu H. L., Chen C. C., Chen Y. G., and Mueller K. J.: The influence of sediment cover variability on long-term river incision rates: An example from the Peikang River, central Taiwan, J. Geophys. Res., 116, F03016, doi:10.1029/2010JF001933, 2011.

Zhang, L., Parker, G., Stark, C. P., Inoue, T., Viparelli, E., Fu, X., and Izumi, N.: Macro-roughness model of bedrock–alluvial river morphodynamics, Earth Surf. Dynam., 3, 113–138, https://doi.org/10.5194/esurf-3-113-2015, 2015.